PROGNOSTICS OF DAMAGE ACCRUAL IN SSL LUMINAIRES AND DRIVERS SUBJECTED TO HTSL ACCELERATED AGING

Pradeep Lall
Auburn University
Department of Mechanical Engineering and
NSF Center for Advanced Vehicle and
Extreme Environmental Electronics, (CAVE^3)
Auburn, AL 36849
Tele: (334) 844-3424
E-mail: lall@auburn.edu

Peter Sakalaukus
Auburn University
Department of Mechanical Engineering and
NSF Center for Advanced Vehicle and
Extreme Environmental Electronics, (CAVE^3)
Auburn, AL 36849

Lynn Davis
RTI International
Research Triangle Park, NC

ABSTRACT

This paper will show an investigation of off-the-shelf luminaires with the focus on the LED electronic drivers, specifically the aluminum electrolytic capacitors (AECs), that have been aged using high temperature shelf life (HTSL) testing of 135°C in order to prognosticate the remaining useful life of the luminaires. Luminaires have the potential of seeing excessive temperatures when being transported across country or being stored in non-climate controlled warehouses. They are also being used in outdoor applications in desert environments that see little or no humidity but will experience extremely high temperatures during the day. This makes it important to increase our understanding of what effects being stored at high temperatures for a prolonged period of time will have on the usability and survivability of these devices. The U.S. Department of Energy has made a long term commitment to advance the efficiency, understanding and development of solid-state lighting (SSL) and is making a strong push for the acceptance and use of SSL products. In this work, the four AECs of three different types inside each LED electronic driver were studied. The change in capacitance and the change in equivalent series resistance (ESR) of the AECs were measured and considered to be a leading indication of failure of the LED system. These indicators were used to make remaining useful life predictions to develop an algorithm to predict the end of life of the AECs. The luminous flux of a pristine downlight module was also monitored using each LED electronic driver that was subjected to HTSL through the progression of the testing to determine a correlation between the light output of the lamp and the failing components of the LED electronic driver. Prognostic and Health Management (PHM) is a useful tool for assessment of the remaining life of electrical components and is demonstrated for AECs in this work.

KEY WORDS

Prognostics, Solid-State Lighting, Electrolytic Capacitors

MOTIVATION

The U.S. Department of Energy (DOE) has made a long-term commitment to advance R&D breakthroughs in efficiency and performance of solid-state lighting (SSL). SSL technology has the potential to reduce the U.S. lighting energy usage in half and produce large savings. The DOE has developed a comprehensive national strategy that encompasses Basic Energy Sciences, Core Technology Research, Product Development, Manufacturing Research and Development (R&D) Initiative, Market Development Support, SSL Partnerships, and Standards Development. [1]

INTRODUCTION

Luminaires are beginning to replace today's incandescent light bulbs and are becoming more prevalent in everyday applications. They are potentially being used in outdoor applications in dry desert environments that see little or no humidity and have the possibility of being transported across country and stored in non-climate controlled trucks and warehouses. Luminaires subjected to a high temperature shelf life for a prolonged period of time may see premature failure of the individual components, specifically that of an aluminum electrolytic capacitor (AEC). AEC degradation may cause the electrical drivers to fail completely due to a current surge or produce an undesirable light output of the light emitting diodes (LEDs). This can potentially erode a manufactures profit margin due to warrantied replacement of the luminaire. AECs are considered the "weakest link" out of all the components that make up the electrical driver studied in this work.

An AEC is a type of capacitor that uses an electrolyte to achieve a larger capacitance per unit volume compared to traditional capacitors. They are used in high current and low frequency electrical circuits, such as an LED electrical driver, and are needed to help convert AC power to DC power [2]. An AEC is composed of a cathode aluminum foil, electrolytic paper, liquid electrolyte and a dielectric [3] [4]. The capacitance can be calculated by knowing the dielectric constant, surface area of the dielectric and the thickness of the dielectric [3] [4] [7]. The ESR can be found by summing the electrolytic resistance, dielectric loss and the electrode resistance using equations outlined in the literature [3] [5] [6] [7]. In this work, the ESR and capacitance were measured directly using a handheld LCR meter.

The predominant failure mechanism of the AEC is the loss of the liquid electrolyte through dissipation and decomposition. Liquid electrolyte loss can be attributed to an elevated ambient temperature, electrochemical reactions at the dielectric layer or diffusion through the seal [5] [7]. This will lead to a drift of the electrical parameters of the AEC (i.e. capacitance and ESR). If an AEC is kept at an elevated ambient temperature for a prolonged period of time causing liquid electrolyte degradation, then the capacitance will decrease and the ESR will increase [3] [4] [5] [6] [7] [8] [9] [10] [11] [12] [13] [15].
Therefore, this makes capacitance and ESR excellent leading indicators to monitor the health of an AEC. This along with the luminous flux or light output of the LED gives great insight on the health of the entire luminaire system.

Prognostic health management (PHM) is a useful tool to assess the remaining useful life of an electrical component such as an AEC using leading indicators of failure. PHM research has been published on AECs and LED packages using a variety of techniques to determine the remaining useful life (RUL) for an assortment of test conditions. One publication studied the effects of electrical overstress accelerated aging on AECs. The ESR and capacitance values were estimated from the capacitor impedance frequency response and a lump parameter model, respectively, and used in conjunction with a Kalman filter to determine the RUL of the AECs [15]. Euclidean and Mahalanobis distance measuring techniques have been used to assess the RUL of a LED package subjected to accelerated voltage conditions based off the degradation in the luminous flux [16]. Three components of a Switching Mode Power Supply: MOSFETs, diodes and AECs have been studied using the theory of Physics of Failure. The values of each component were estimated with the equations outlined in the literature and were used with a linear regression model to make RUL predictions [17]. The ESR and capacitance of AECs in an uninterruptible power supply has been studied. The values were estimated using current and voltage measurements of the power supply and used in conjunction with a Least Squares algorithm to extrapolate RUL of the AECs [18].

In this work, the ESR and capacitance has been measured directly for AECs subjected to a HTSL test of 135 °C. The ability to assess damage accrual in AECs before failure and prognosticate remaining useful life is essential to understanding the life time of the luminaire itself. A Kalman Filter was used as a recursive algorithm to estimate the true state of the AECs based off the collected data [19] [20] [21]. The luminous flux was also recorded to investigate possible leading indications of failure in the driver.

TEST VEHICLE

The test vehicle for this work was a Philips Fortimo LED DLM system which included a Philips Fortimo downlight lamp, a Philips Xitanium electrical driver and a cable to connect the lamp to the electrical driver. The power cords to connect the electrical driver to the main power supply were constructed in-house. The pristine assembly shown in Figure 1 was used to calculate the luminous flux of the downlight.

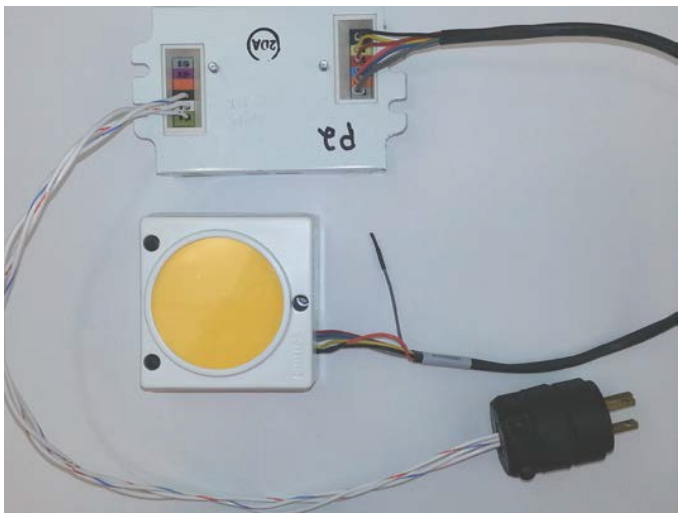

Figure 1: The Philips Fortimo LED DLM System.

Each sample set of AECs were taken from a single Philips Xitanium electrical driver. These AECs were removed to directly measure the capacitance and ESR. Figure 2 depicts the circuit board of a single Xitanium driver with the four AECs removed.

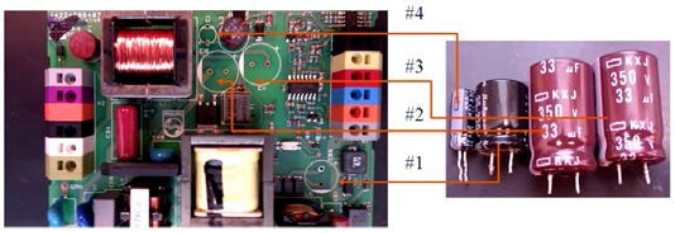

Figure 2: AECs Removed from the Philips Xitanium Driver.

Each Xitanium electrical driver consisted of four AECs of three various types. The AEC characteristics are given in Table 1.

Table 1: AEC Characteristics.

AEC #	Endurance @ 105 °C [Hrs.]	Temperature Range [°C]	Rated Voltage [Vdc]	Capacitance [µF]
1	8k – 10k	-40 – 105	35	220
2 & 3	10k – 12k	-40 – 105	350	33
4	4k – 5k	-40 – 105	50	22

TEST ENVIRONMENT

The removed AECs and the remaining portion of the Philips Xitanium driver were kept in a Thermotron thermal chamber at 135 °C for the duration of the test. The components were removed from the chamber and allowed to cool to room temperature for approximately one hour before measurements were taken. The ESR and capacitance of each AEC was measured directly using an Agilent U1733C handheld LCR meter.

Luminous flux calculations were also carried out for each sample set on the same pristine Philips Fortimo LED downlight following the IES LM-79-08 standard [22]. The AECs were connected to its Philips Xitanium driver through a bread board. The light output leads of the electrical driver were connected to another portion of the bread board which allowed easy switching between drivers to record the radiant flux values needed to calculate the luminous flux. An USB4000 Spectrometer from Ocean Optics, SpectraSuite software and a one meter integrating sphere were used to precisely obtain the radiant flux data of the downlight for each driver. Figure 3 illustrates the luminous flux setup.

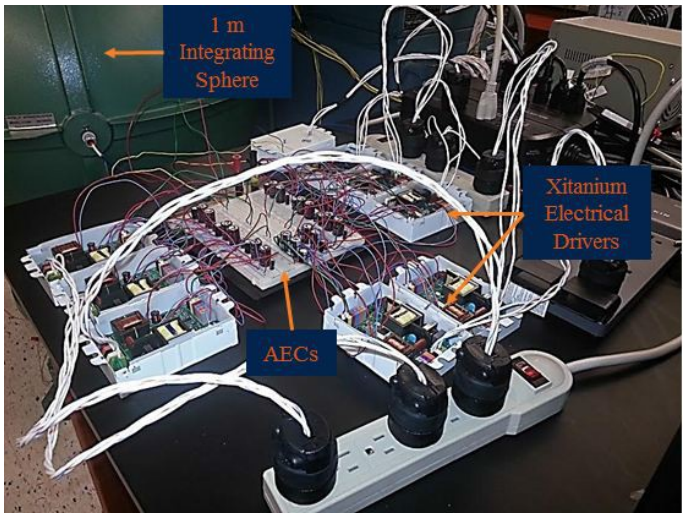

Figure 3: Luminous Flux Measurement Setup.

IES LM-79-08

The total spectral radiant flux, $\phi_{test}(\lambda)$, of a SSL product under test is obtained by comparison to the total spectral radiant flux of a reference standard [22]. It can be found using the following equation:

$$\Phi_{test}(\lambda) = \Phi_{m}(\lambda) \oplus \alpha_{CCF} \quad (1)$$

The measured spectral radiant flux, $\phi_{m}(\lambda)$, of the test lamp is computed using the SpectraSuite software. The self-absorption factor, α_{CCF}, can be found using an auxiliary lamp in conjunction with the test lamp and a reference lamp. It is determined using the spectrometer measurements of the auxiliary lamp with the test lamp and then with the reference lamp. The ratio of the measurements of the auxiliary lamp with the reference lamp divided by the auxiliary lamp with the test lamp will produce the self-absorption factor.

The total luminous flux, ϕ_{test}, in lumens [lm] of the SSL product under test can now be found using the total spectral radiant flux found from equation (1) with equation (2) [22].

$$\Phi_{test} = K_m \oplus \int_{380}^{780} \Phi_{test}(\lambda) \oplus V(\lambda) \oplus d\lambda \quad (2)$$

$$K_m = 683 \, lm/W$$

The spectral luminous efficiency function for photopic vision, V(λ), is well documented in literature and K_m is the maximum spectral luminous efficiency [23].

KALMAN FILTERING

The discrete Kalman filter estimates the instantaneous state of a linear dynamic system that is perturbed by noise [19]

[20] [21]. A Kalman filter was used to prognosticate the

remaining useful life (RUL) of aluminum electrolytic capacitors using two different leading indicators or feature vectors: the change in capacitance (ΔC) and the change in ESR (ΔESR). The RUL found from both feature vectors was compared to determine which leading indicator is best for investigating the health management of the system. The system state has been described in state space form using the measurement of the feature vector, the estimated velocity of the feature vector and the estimated acceleration of the feature vector. The system state at each future time has been computed based on the state space at the preceding time step, system dynamics matrix, control vector, control matrix, measurement matrix, measured vector, process noise and measurement noise. Figure 4 represents the data-flow through the system, where u is the control vector or input for the system, w is process noise, x is the state space vector, H is the measurement matrix, v is the measurement noise, z is the measured state, T is a time delay, and F is the system dynamics matrix.

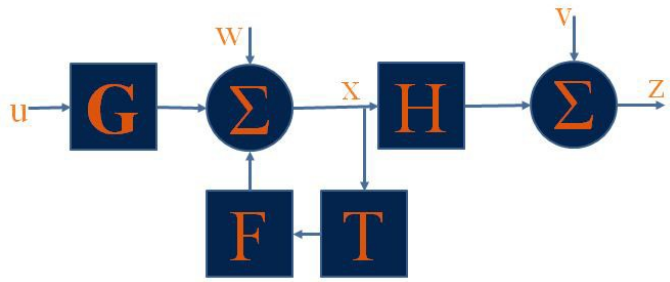

Figure 4: State Space Representation of a System.

In order to apply the Kalman filter, the signal response must be described by a set of differential equations [20]. Therefore, the equivalent Kalman Filter equation for state space representation with the presence of process noise and measurement noise is shown in equation (3) with the final version of the Kalman Filter equation illustrated in equation (4).

$$\hat{x}=F\oplus x+G\oplus u+w \tag{3}$$

$$\hat{x}_k=\Phi\oplus\hat{x}_{k-1}+G_k\oplus u_{k-1}+K_k\oplus(z_k-H\oplus\Phi\oplus\hat{x}_{k-1}-H\oplus G_k\oplus u_{k-1}) \tag{4}$$

$$z_k=H\oplus x_k+v_k \tag{5}$$

The variable $\hat{x}_k$ is the Kalman Filter system state estimate at the k^{th} time step, and x_k is the actual system state at the k^{th} time-step and G_k is the control matrix.

$$M_k=\Phi\oplus P_{k-1}\oplus\Phi^T+Q_k \tag{6}$$

$$K_k=M_k\oplus H^T\oplus(H\oplus M_k\oplus H^T+R_k)^{-1} \tag{7}$$

$$P_k=(I-K_k\oplus H)\oplus M_k \tag{8}$$

The variable M_k is the covariance of errors in state estimates before update, ϕ_k is the fundamental matrix which represents the system dynamics, Q_k is the discrete process noise matrix, K_k is the Kalman gain, H is the measurement matrix, and P_k is the covariance matrix representing errors in the state estimate after an update. R_k is the discrete measurement noise matrix and has been used as a device for telling the filter that we know that the filter's model of the real world is not precise. The diagonal elements of P_k represent variance of the true state minus the estimated state. M_k is sometimes referred to as the a priori covariance matrix and P_k may be referred to as the posterior covariance matrix.

Since the feature vectors used for prognostication of the system health are usually not constant nor a straight line, the zeroth and first order systems were ruled out and a second order system was used for the representation of the system state evolution with progression of underlying damage. The choice of the second order filter was also influenced by the general observation that feature vectors evolve non-linearly and generally accelerate towards the end of life. The rate of evolution of a second order system can be represented as follows:

$$\begin{bmatrix}\dot{x}\\ \ddot{x}\end{bmatrix}=\begin{bmatrix}F\end{bmatrix}\oplus\begin{bmatrix}x\\ \dot{x}=0\end{bmatrix}\qquad\begin{bmatrix}0 & 1 & 0\\ 0 & & 1\end{bmatrix}\oplus\begin{bmatrix}x\\ \dot{x}\end{bmatrix} \tag{9}$$

$$\begin{bmatrix}\dot{x}\\ \ddot{x}\end{bmatrix}=\begin{bmatrix}0 & 0 & 0\end{bmatrix}\begin{bmatrix}\ddot{x}\end{bmatrix}$$

The fundamental matrix has been computed from the Taylor series expansion of the system dynamics matrix, F, as follows:

$$\Phi(t)=e^{F\oplus t}=I+F\oplus t+\frac{F^2\oplus t^2}{2!}+\frac{F^n\oplus t^n}{n!} \tag{10}$$

$$\begin{bmatrix}1 & 0 & 0\\ 0 & 1 & 0\\ 0 & 0 & 1\end{bmatrix}+\begin{bmatrix}0 & 1 & 0\\ 0 & 0 & 1\\ 0 & 0 & 0\end{bmatrix}t+\begin{bmatrix}0 & 0 & 1\\ 0 & 0 & 0\\ 0 & 0 & 0\end{bmatrix}\frac{t^2}{2!} \tag{11}$$

The Kalman gains are computed while the filter is operating from a set of recursive matrix equations called the Riccati equations [20]. The Riccati equations are represented as:

$$\Phi(t) = \begin{bmatrix} 1 & T_s & \frac{T_s}{2} \\ 0 & 1 & T_s \\ 0 & 0 & 1 \end{bmatrix} \quad (12)$$

A model based on the accrued damage of the system has not been used because the inputs to the system are not always known or measurable and cannot be assumed to always be constant or known in advance. Therefore, the feature vectors based on ΔC and ΔESR have been used as system inputs to estimate the system state**.** The first and second derivatives of each feature vector from the direct measurement of each AEC have been computed to estimate the state of each feature vector at future time-steps. The system state vector is represented as $x_k = [x \quad \dot{x} \quad \ddot{x}]^T$, where x is ΔC or ΔESR, $\dot{x}$ is the ramp rate of each feature vector and $\ddot{x}$ is the second derivative with respect to time of each feature vector. The state vector evolution is represented as follows:

$$\begin{bmatrix} x_{k+1} \\ \dot{x}_{k+1} \\ \ddot{x}_{k+1} \end{bmatrix} = \begin{bmatrix} 1 & T_s & \frac{T_s}{2} \\ 0 & 1 & T_s \\ 0 & 0 & 1 \end{bmatrix} \begin{bmatrix} x_k \\ \dot{x}_k \\ \ddot{x}_k \end{bmatrix} \quad (13)$$

The uncertainty of each prediction was quantified using the posterior error covariance. The extrapolation of the estimated state into the future to determine the RUL was accomplished by using the state evolution equation to iteratively solve the intersection of the underlying physics models. The parameters are estimated from the Kalman filter. Two simple models were used to describe the collected data: a linear model for Δc and an exponential model for ΔESR. This is shown in equations (14) and (15), respectively.

$$f(t) = a + b \oplus t_{fn} \quad (14)$$

$$f(t) = a \oplus \exp(b \oplus t_{fn}) \quad (15)$$

$$a = x$$

$$b = \ddot{x} / \dot{x}$$

The variable x is the state variable in the state space, t_{fn} is the estimate of the failure time at the time-step n and x_f is the failure threshold for the state variable. The estimate of the failure time is updated during the evolution of the state-space vector with the underlying damage. The Kalman filter outlined above was used to prognosticate the remaining useful life of the AECs using both feature vectors.

PHM

The average of each capacitor's ESR and capacitance at each time step has been used for the reliability analysis. The leading indicators of failure are trending in the correct direction. An ample amount of data has been collected and used to train the model to accurately make predictions of the feature vectors. The graphs of the ΔESR and ΔC of each capacitor are shown in Figure 5, Figure 6, Figure 7 and Figure 8, respectively. The noise threshold has already been eliminated for each data set with the first datum point given a value of one for 100%.

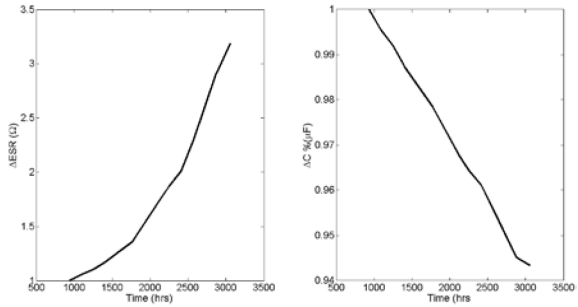

Figure 5: The Average ΔESR and ΔC for AEC One.

$$a = x \tag{14}$$

$$b = \dot{x}$$

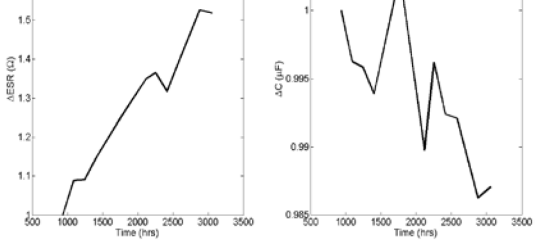

Figure 6: The Average ΔESR and ΔC for AEC Two.

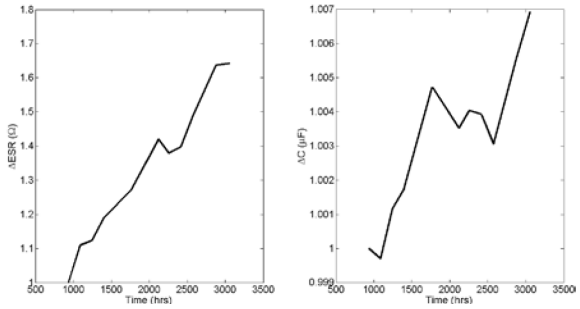

Figure 7: The Average ΔESR and ΔC for AEC Three.

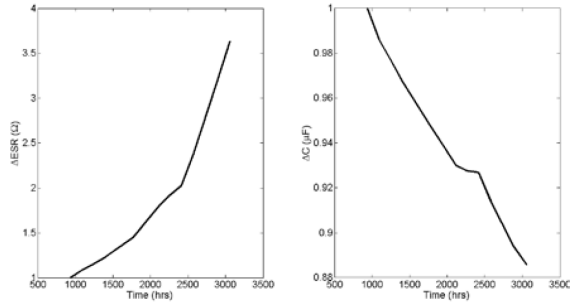

Figure 8: The Average ΔESR and ΔC for AEC Four.

The failure threshold for the luminaire has been taken as 70% of the luminous flux or the L70 value [22]. The pristine luminous flux value of the luminaire under test is 2000 lm ± 10%. As of now, the L70 value of the luminaire has not been reached and the luminaire is still producing a pristine reading. The average luminous flux value for each measurement time is shown in Figure 9.

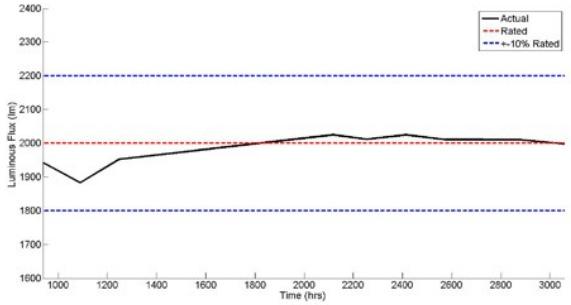

Figure 9: Average Luminous Flux of the Luminaire.

Based off of Figure 9, the calculated luminous flux of the luminaire is almost identical to that of the rated luminous flux value. Therefore, no correlation between ΔESR and ΔC can be made with the luminous flux calculations because the luminaire hasn't deviated outside of the pristine range. Since the luminaire is still "pristine", the AECs have not "failed" in the traditional sense even though there is some measured degradation occurring with the AECs.

Figure 6 and Figure 7 shows no discernible change in the ΔESR and ΔC measurements of AECs #2 and #3. Both of these AECs are reading at approximately 100% at each collected ΔC value with only a slight change in ΔESR. Looking at Figure 5 and Figure 8, it is observed that AECs #1 and #4 are trending almost identically. After careful study of the electrical driver's circuit diagram, it has been determined that AEC #1 will have the greatest effect on the luminous flux output compared to AEC #4. By treating AEC #1 as the weakest link out of all four AECs, the overall health of the luminaire can be monitored and end of life can be predicted at any desired failure threshold. The ΔESR and ΔC of AEC #1 has been used to train a Kalman filter algorithm to show how robust the algorithm will work for this luminaire's components. The collected data was also used to make end of life predictions for this luminaire. Since the final time till failure of AEC #1 is unknown, the extrapolations forward in time were carried out for ten times the final collected time value of 3057.6 hours. Figure 10 shows the collected ΔESR data, the filtered data and the forecasted predictions at each data point.

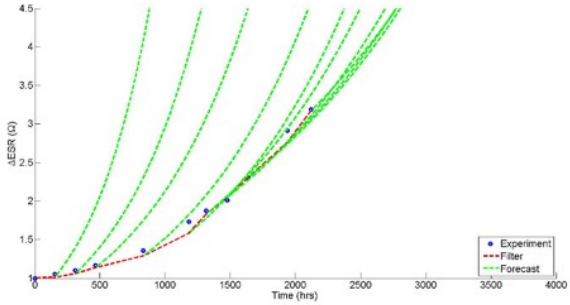

Figure 10: Kalman Filter Plot of ΔESR for Capacitor One.

The Kalman filter produced an output that mimics the collected ΔESR data reasonably well. The model forecasted the ΔESR towards the end of life at each collected data point. The extrapolations began to converge towards a common point at the last three data points. This shows that the model has been reasonably trained and has started to make what seem to be accurate predictions. The same graph has been produced for ΔC. Figure 11 shows the collected ΔC data, the filtered data and the forecasted predictions at each data point.

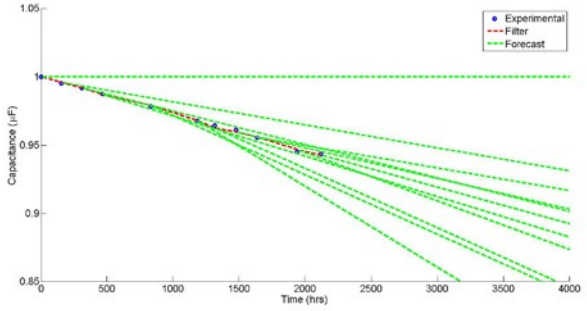

Figure 11: Kalman Filter Plot of ΔC for Capacitor One.

The Kalman filter produced an output that is closer to the collected ΔC data when compared to that of the ΔESR filtered data in Figure 10. However, the model's forecasted ΔC does not converge at any point in the extrapolations. This shows that more data is needed to train the model better to accurately predict the ΔC.

PROGNOSTICS METRIC

The experimental value of time to failure is typically known after the completion of accelerated testing. A comparison of the actual life of the component versus the predicted life can then be made to validate the model and show the robustness of the PHM algorithm. Since the collection for this test is ongoing, the actual end of life of the system is not known. Therefore, in order to validate this model, the collected data was used to show how well the algorithm has worked thus far with the last datum point used as a pseudo end of life.

The validation process follows one of the algorithm assessment metrics proposed in literature [24] [25] [26] [27]. The alpha-lambda performance metric was used for both the ΔESR and ΔC to show how well the Kalman filter algorithm has predicted the RUL. The RUL of AEC #1 for both the ΔESR and ΔC data has been determined using the pseudo end of life. This compares the actual RUL against the predicted RUL. Figure 12 and Figure 13 illustrate the alpha-lambda performance metrics for ΔESR and ΔC, respectively.

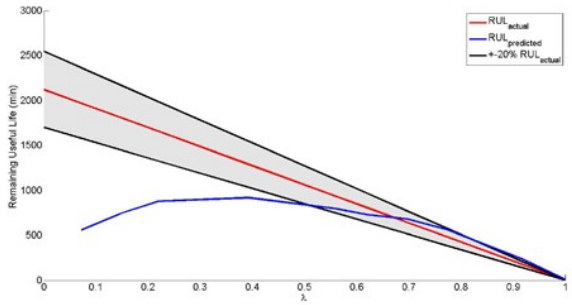

Figure 12: Alpha-Lambda Performance Metric for ΔESR.

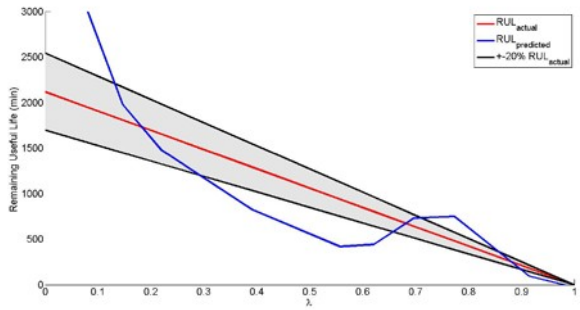

The gray shaded area in the alpha-lambda graphs is called the alpha bounds. It provides a region to describe the accuracy of the algorithm and is taken at ± 20 % of the actual RUL. If the predicted RUL falls within the alpha bounds, then it is taken as a correct prediction. Lambda is defined as the normalized time and is calculated as $\lambda = t/t_{EOL}$ where t is

Figure 13: Alpha-Lambda Performance Metric for ΔC.

the present time, and t_{EOL} is the time to the end of life. Normalized time is plotted on the x-axis. When lambda equals one, the part has "failed".

In Figure 12, the Kalman filter algorithm grossly under predicted the RUL in the beginning and never over predicts the RUL. Typically, it is better to under predict than to over predict. The predicted RUL starts to converge towards the actual RUL and stays within the alpha bounds at about half way through the collected data. This means that the algorithm has worked reasonably well at forecasting the ΔESR. This also shows that this leading indicator is useful for monitoring the health of the luminaire to predict failure.

Figure 13 shows oscillations in the prediction. The Kalman filter algorithm under predicts and over predicts the RUL. It also does not converge toward the actual RUL. The algorithm used with the ΔC data needs more datum points to possibly make accurate predictions. Therefore, this leading indicator is not a good choice for monitoring the health of the luminaire at this time.

SUMMARY AND CONCLUSIONS

This paper has shown an investigation of a Philips Fortimo LED DLM system with the focus on the LED electronic drivers, specifically the aluminum electrolytic capacitors (AECs) inside the electrical drivers. The electrical drivers were aged using high temperature shelf life (HTSL) testing at 135°C. The collected data was used in conjunction with a Kalman filter algorithm to determine the RUL of the AEC in order to monitor the health of the luminaire.

The four AECs of three different types inside each LED electronic driver were removed from the driver to obtain the exact capacitance and ESR values using a handheld LCR meter. They were then placed back into the electrical drivers to calculate the luminous flux of the luminaire.

ΔESR and ΔC were considered leading indicators of failure and were used to study the reliability of the luminaire using a Kalman filtering algorithm. AEC #1 was determined to be the weakest link compared to the other AECs and was used to make remaining useful life predictions of the luminaire for the collected data.

It was shown that the ΔESR and the Kalman filter algorithm produced RUL predictions the converged towards the same value. It was validated and proven acceptable using the alpha-lambda performance metric. The ΔC data did not converge towards the same end of life predictions using the

collected data. Therefore, the ΔESR is a better leading indicator for predicting the RUL compared with the ΔC.

The collection of ΔESR and ΔC data is ongoing and will continue until complete failure. With the continued collection of data, the Kalman filter algorithm can be better trained to make RUL predictions and validated with other prognostics metrics.

Additional testing will be completed to compile a larger data set. This will help in fine tuning the Kalman filter algorithm, as well as, the experimental setup. Also, the Newton-Raphson's method will be used to aid in the production of a more robust underlying physics model for the calculation of the remaining useful life.

ACKNOWLEDGMENTS

The work presented here in this paper has been supported by a research grant from the Department of Energy under Award Number DE-EE0005124.

REFERENCES

[1] U.S. Department of Energy: Energy Efficiency & Renewable Energy. "Solid-State Lighting." *Building Technology Programs.* DOE, 9 April 2012. Web. 5 May 2012.

[2] Georgiev, Alexander M. *The Electrolytic Capacitor.* New York: Murray Hill Books, 1945.

[3] Rubycon Corporation, *Technical Notes for Electrolytic Capacitor*.

[4] Nichicon Inc. *General Descriptions of Aluminum Electrolytic Capacitors.* 2002.

[5] Han, L. and Narendran, N. "Developing an Accelerated Life Test Method for LED Drivers." *Proc. of SPIE: 9th International Conference on Solid State Lighting.* 2009.

[6] Harada, K., Katsuki, A. and Fujiwara, M. "Use of ESR for Deterioration Diagnosis of Electrolytic Capacitor." *IEEE Trans. on Power Electronics.* Vol. 8, pp. 355-361, Oct., 1993.

[7] Jianghai Europe GmbH. *Electrolytic Capacitor Lifetime Estimation*. 2010.

[8] Gasperi, M.L. "Life Prediction Model for Aluminum Electrolytic Capacitors." *IEEE Industry Applications Conf.* Vol. 3, pp. 1347-1351, Oct., 1996.

[9] BHC Components. *Aluminum Electrolytic Capacitor Application Notes*. 2002.

[10] Sankaran, V.A., Rees, F.L., and Avant, C.S. "Electrolytic Capacitor Life Testing and Prediction." *IEEE Industry Applications Conf.* Vol. 2, pp. 1058-1065, Oct., 1997.

[11] Stevens, J.L., Shaffer, J.S. and Vandenham, J.T. "The Service Life of Large Aluminum Electrolytic Capacitors: Effects of Construction and Application." *IEEE Trans. on Industry Applications.* Vol. 38, Issue 5, pp. 1441-1446, Oct. 2002.

[12] Panasonic Industrial Company. *Aluminum Electrolytic Capacitors*. 2008.

[13] Cornell Dubilier Electronics Inc. *Application Guide, Aluminum Electrolytic Capacitors.* 2000.

[14] Ma, H., Wang, L. "Fault Diagnosis and Failure Prediction of Aluminum Electrolytic Capacitors in Power Electronic Converters." *Industrial Electronics Society, 2005. IECON 2005. 31st Annual Conference of IEEE*, pp. 6, Nov. 6, 2005.

[15] Celaya, J.R., Kulkarni, C., Biswas, G., Saha, S. and Goebel, K. "A Model-based Prognostics Methodology for Electrolytic Capacitors Based on Electrical Overstress Accelerated Aging." *Annual Conf. of the PHM Society.* 2011.

[16] Sutharssan, T., Bailey, C., Stoyanov, S. and Rosunally, Y. "Prognostics and Reliability Assessment of Light Emitting Diode Packaging." *IEEE International Conf. on Electronic Packaging Technology & High Density Packaging.* 2011.

[17] Zhou, Y., Li, X., Ye, X. and Zhai, G. "A Remaining Useful Life Prediction Method Based on Condition Monitoring for LED Driver." *IEEE Prognostics & System Health Management Conf.* 2012.

[18] Abdennadher, K., Venet, P., Rojat, G., Retif, J.M. and Rosset, C. "A Real-Time Predictive-Maintenance System of Aluminum Electrolytic Capacitors Used in Uninterrupted Power Supplies." *IEEE Transactions on Industry Applications.* pp. 1644-1652, Vol. 46 #4, 2010.

[19] Grewal, M. S. and Andrews, A. P. Kalman Filtering: Theory and Practice Using MATLAB, 2nd ED. New York: John Willy & Sons Inc., 2001.

[20] Zarchan, P. and Musoff, H. Fundamentals of Kalman Filtering: A Practical Approach. Virginia: Volume 190 Progress in Astronautics and Aeronautics, 2000.

[21] Balakrishnan, A. V. Kalman Filtering Theory (Series in Communication and Control Systems). New York: Optimization Software, 1987.

[22] IES Illuminating Engineering Society. *Approved Method: Electrical and Photometric Measurements of Solid-State Lighting Products.* 2008.

[23] DeCusatis, Casimer. *Handbook of Applied Photometry.* New York: AIP Press, 1997.

[24] Saxena, A., Celaya, J., Saha, B., Saha, S., and Goebel, K. "Evaluating Algorithm Performance Metrics Tailored for Prognostics." *IEEE Aerospace Conference*. 2008.

[25] Saxena, A., Celaya, J., Balaban, E., Saha, B., Saha, S., Goebel, K. and Schwabacher, M. "Metrics for Evaluating Performance of Prognostic Techniques." *Intl. Conf. on Prognostics and Health Management*. 2008.

[26] Saxena, A., Celaya, J., Saha, B., and Goebel, K. "Evaluating algorithm performance metrics tailored for prognostics." *IEEE Aerospace conference*. 2009.
[27] Saxena, A., Celaya, J., Saha, B., Saha, S., and Goebel, K. "On Applying the Prognostics Performance Metrics." *Annual Conference of the PHM Society*. 2009.

NOMENCLATURE

HTSL	High Temperature Shelf Life
ESR	Equivalent Series Resistance
RUL	Remaining Useful Life
AEC	Aluminum Electrolytic Capacitors
PHM	Prognostics and Health Management
ΔC	Change in Capacitance
ΔESR	Change in Equivalent Series Resistance
$\phi_{test}(\lambda)$	Test Lamp Radiant Flux
$\phi_{m}(\lambda)$	Test Lamp Measured Radiant Flux
α_{CCF}	Self-Absorption Factor
K_m	Maximum Spectral Luminous Efficiency
$V(\lambda)$	Spectral Luminous Efficiency Function
ϕ_{test}	Test Lamp Luminous Flux
x	State Space Vector
F	System Dynamics Matrix
u	Control Vector
w	Process Noise Vector
z	Measurement Vector
H	Measurement Matrix
v	Measurement Noise Vector
I	Identity Matrix
Φ	Fundamental Matrix
T_s	Sampling Time
Φ_k	Discrete Fundamental Matrix
x_k	Discrete State Space Vector
z_k	Discrete Measurement Vector
v_k	Discrete White Noise Measurement Vector
R_k	Discrete Measurement Noise Vector
G_k	Kalman Control Matrix
M_k	Covariance Matrix
K_k	Kalman Gain Matrix
P_k	Updated Covariance Matrix
Q_k	Discrete Process Noise Matrix
$\hat{x}_k$	State Space Vector Estimation
k	Time Step
t_{eol}	Time at End of Life